

PECULIARITIES OF SILVER PHOTODISSOLUTION IN $(GeS_4)_x(AsS_3)_{x-1}$ GLASSY FILMS

D. Tsiulyanu , I. Stratan and N. Piletchi

Department of Physics, Technical University of Moldova
tsiu@molddata.md; ionstratan@gmail.com; pil-nata-@mail.ru

Abstract. *The kinetics of the photodissolution (PD) of Ag into glassy $(GeS_4)_x(AsS_3)_{x-1}$ films has been studied by monitoring the changes that occur in their optical transmission of weakly absorbed broadband light. It was shown that the kinetics profiles comprise two consecutive linear steps followed by a quasi – parabolic tail. The PD rate and the amount of adopted Ag on the first step were found (except of GeS_4) not to depend on glass composition. This result was ascribed to provide evidence for a preferential and direct interaction of Ag with free sulfur at the interface. The rate of PD on the second linear step exhibits a compositional maximum around $(GeS_4)_{0.33}(AsS_3)_{0.67}$, being by two orders of magnitude higher than the rate for GeS_4 . The revealed compositional dependences are qualitatively attributed to the fact that only some, very specific glassy compositions being Ag photodoped yield a homogeneous material.*

Keywords: *glassy chalcogenides, photodissolution, kinetics.*

I. Introduction

PD of the metals (e.g. Ag) in chalcogenide glasses (*GhG*), being to all appearances a unique property of these materials, is widely discussed in the science literature (see an extensive review ref. [1]). It was pointed out that PD process is due both to an inhomogeneous chemical photo-induced reaction, which results in formation of a solid mixture $GhG:Ag$ with a high ionic conductivity (superionic conductor) [2] and diffusion of Ag^+ ions through this superionic layer [2,3]. Recently have been suggested [4] that the PD starts at the interface by chemical reaction between homopolar chalcogen (S-S) segments and neutral Ag forming Ag_2S . Then Ag_2S reacts with “wrong” bonds (such as As-As) converting the neutral silver into Ag^+ ions, which are able to diffuse deeper in the chalcogenide film. As all listed mechanisms of PD overlaps, it is not easy to distinguish between them. In this context the compositional features of this phenomenon are of paramount importance.

In the present work we report the influence of composition of *ChG* on silver PD process, by transition from threefold coordinated As-based backbone to fourfold coordinated Ge-based structure using ternary system $(GeS_4)_x(AsS_3)_{x-1}$.

II. Results and discussion

The glassy alloys were prepared by melt-quenching method of pure (99, 99%) As, S and Ge in quartz ampoules evacuated up to $5 \cdot 10^{-5} Torr$. Seven compositions, which are listed in Table 1, have been synthesized. Thin films have been prepared by thermal “flash” evaporation of priority-synthesized materials onto Pyrex glass substrates, at room temperature. The evaporation was performed from a tantalum boat at the working pressure of $10^{-4} Pa$. The thickness of the films was around 1mm and the area of deposition being about $1,5 cm^2$. The silver films were deposited also by

thermal evaporation in vacuum on top of the chalcogenide films, immediately (breaking the vacuum) after their preparation. The thickness of the silver film was kept constant of about 50 nm .

Table 1. Composition, and some physical parameters of $(GeS_4)_x(AsS_3)_{1-x}$ glasses.

Nr.	Composition [x]	E_g , eV	r , kg/m ³	Concentration, mol/cm ³ · 10 ⁻²			$k \cdot 10^{13}$, cm ² s ⁻¹
				[AsS] _{3/2}	[GeS] _{4/2}	[S-S] _{2/2}	
1	0	2.75	2677.6	1.57	0	1.17	2.80
2	0.17	2.69	2632.9	1.30	0.26	1.23	2.13
3	0.33	2.66	2611.9	0.96	0.48	1.2	3.5
4	0.5	2.61	2571.7	0.69	0.69	1.21	1.42
5	0.67	2.59	2527.8	0.44	0.88	1.23	0.79
6	0.83	2.56	2495.0	0.22	1.08	1.24	0.33
7	1	2.54	2437.9	0	1.22	—	—

PD of silver onto *ChG* was performed by illumination the *Ag* film, lying on the top of the multilayer structure, using the light of a 100W halogen lamp focused by a quartz lens to the side of transparent substrate (Fig.1). The incident power was estimated at the sample surface as 250 mW/cm². Fig. 1 shows schematically the multilayer structure of the sample.

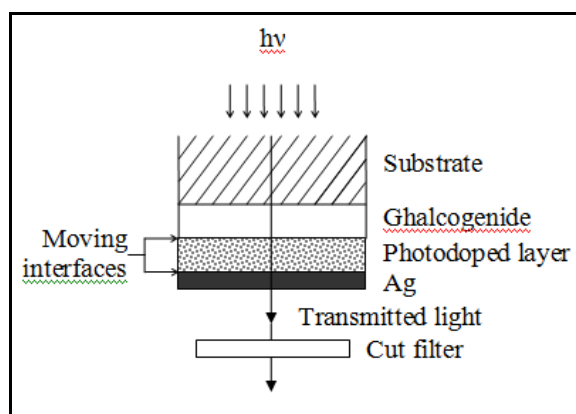


Fig. 1 Schematic cross - section through a sample during the PD process.

There are three well-defined boundaries: 1) substrate / undoped *ChG*; 2) undoped *ChG* / photodoped material (solid electrolyte); 3) photodoped material / *Ag* . During the photodissolution the boundary between photodoped material and undoped *ChG* propagates towards the substrate, but the boundary between photodoped material and *Ag* propagates in opposite direction i.e. towards surface, so that the thickness of both *Ag* layer and undoped *ChG* glass decrease with time.

The instantaneous transmission of unreacted *Ag* layer (T_{Ag}) and that of the whole two-layered *ChG/Ag* structure (T) are interdependent as $T_{Ag} = T/T_0$, where T_0 is the transmission of pure *ChG* layer on glassy substrate. Hence, the PD rate of *Ag* can be estimated by measuring the recovery rate of optical transmission of two-layer structure *ChG/Ag* in IR region of spectrum if the thickness dependence of *Ag* film transmittance is a priori known [5]. Figure 2 shows the optical transmission of the two-layered structure *ChG/Ag* (broadband light $\lambda > 0,65 \mu m$) versus exposure time as PD proceeds.

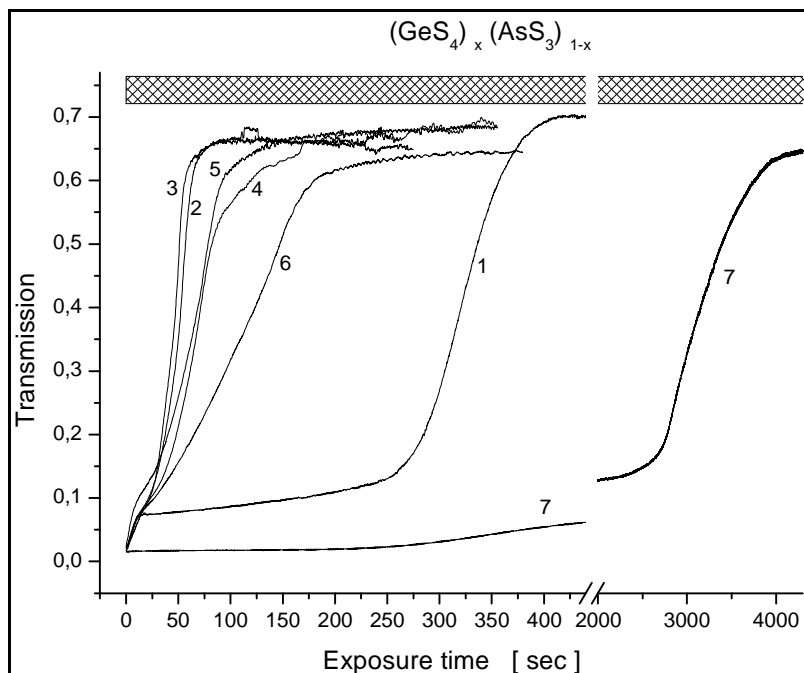


Fig. 2 Transmission of a broadband light $\lambda > 0,65 \mu\text{m}$ of two-layered structures versus exposure time. The numbers of curves correspond to the composition numbers listed in Table 1. The shaded area indicates the transmittance of pure $(\text{GeS}_4)_x(\text{AsS}_3)_{1-x}$ films.

It is seen that independently of composition the transmission of two - layer structure in the region of weakly absorbed light, recovers to that of pure *ChG*, i.e. before deposition of *Ag* layer. Obviously this is due to a decrease of *Ag* layer effective thickness: the absorption coefficient of *Ag* film, is about 10^5 cm^{-1} [6], but even high (~ 60 at. %) *Ag* doped *As-S* or *Ge-S* layers are nearly transparent in this region of spectrum [7]. Except of GeS_4 , a very sharp rising of transmittance was observed at early stage of PD process, which then turns into a composition dependent shoulder, followed by a transition to usual monotonic increasing of transmittance as PD proceeds.

We have calculated and plotted the thickness of unreacted *Ag* film versus exposure time (PD kinetics) applying our experimental data (T_{Ag}) to the thickness dependence of transmission spectra of silver films measured by X. Sun et al. [8].

Figure 3 shows the unreacted *Ag* layer thickness (with displayed error bars) versus exposure time for several compositions of $(\text{GeS}_4)_x(\text{AsS}_3)_{1-x}$ system. For all compositions, except of GeS_4 , three stages of PD kinetics can clearly be distinguished: (I) the first, very sharp step is nearly independent on composition but the thickness of *Ag* layer linearly decreases with exposure time, (II) the second one is a linear shoulder with a slope (the PD rate) strongly influenced by *ChG* composition and the final (III) step exhibits an weak sub linear dependence of thickness change of *Ag* layer on time, particularly observed for GeS_4 .

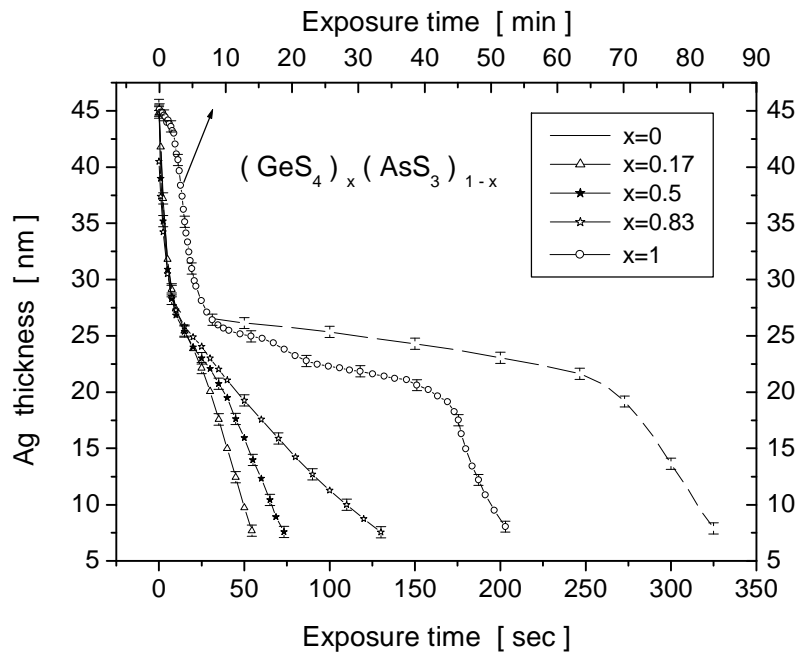


Fig. 3 Decrease of Ag film thickness versus exposure time for several compositions.

It should be mentioned that PD of Ag in GeS_4 was observed in our experiments to exhibit particular behavior. For one thing, it is preceded by a relatively short induction period (Fig.2, curve 7). Further, it precedes very slowly (Fig. 2 and 3) at all stages: 10 - 100 times slower than in any other composition in question, and as a consequence, the first sharp step of PD in GeS_4 does not overlap with similar steps of other compositions.

The segmentation of kinetics curve with non monotonic transition between steps of PD process was reported in our previous paper for glassy As_2S_3 [5], which is a binary stoichiometric compound. The PD rate on the first linear step was found for As_2S_3 strongly to depend on temperature, but at room temperature it exhibits the value of about 0.5 nm/s.

Figure 4a shows the PD rate on the first linear step for the glassy materials applied in the present investigation. As one can follow from this figure the PD rate, being of about 2.0 nm/s is several times higher than for As_2S_3 [5] and, what is more, with except of GeS_4 , the PD rate does not much vary with glass composition.

We assert that the availability of free sulfur in all examined glasses, especially in the form of [S-S] chains (Table 1), explains both the high rate of PD on the first linear step and its weak dependence on composition. In fact, following the model suggested in [7], the silver dissolution starts at the interface by chemical reaction between these segments and neutral Ag as:



The large amount of free sulfur, i.e. [S-S] segments leads to formation of a sufficient amount of As_2S to be connected both in $(Ag_2S)_x(GeS_4)_{1-x}$ and $(Ag_2S)_x(AsS_3)_{1-x}$ glasses. As a result the percolation threshold occurs in the layer at the interface along with its transition to superionic conductivity [9]. Not much difference in the concentration of [S-S]_{2/2} structural units, i.e. in amount of free sulfur (table 1), results in overlapping of kinetics curves on the first stage of PD, as well as in their identical length.

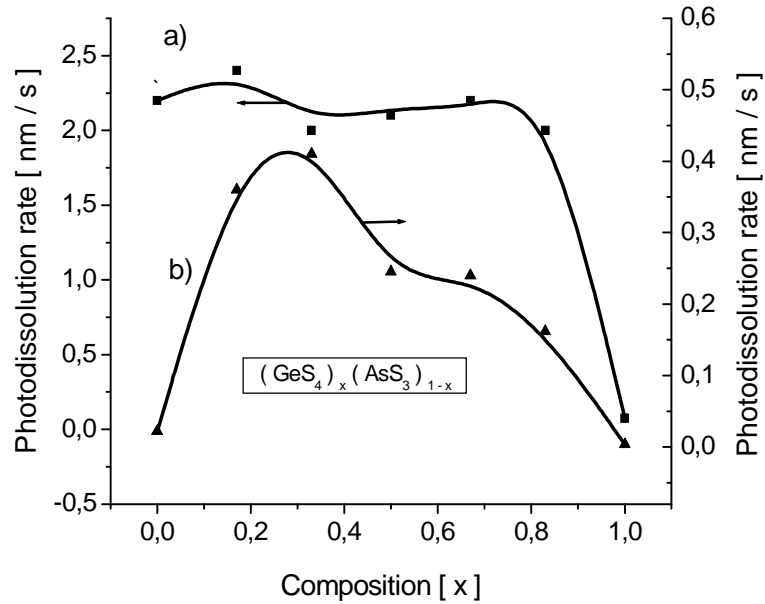


Fig. 4 The PD rate on the first (a) and second (b) linear steps versus glass composition.

The second step of PD kinetics (Figure 3) shows also a linear dependence of the change of Ag thickness on time (the constant rate of PD), but its slope strongly depends on the glass composition. The variation of PD rate with $(GeS_4)_x(AsS_3)_{1-x}$ composition determined from the slope of the second step is shown in Figure 4b. As the GeS_4 content is increased the PD rate increases to a maximum around $(GeS_4)_{0,33}(AsS_3)_{0,67}$ and then falls down. The maximum and minimum rates differ by 20 times.

The constant rate of PD is generally agreed to be determined by reaction between metal and ChG , which occurs simultaneously in two different spatial regions of the sample: (I) absorption of photons by breaking $As(Ge)-S$ bonds that results generation of free holes at the doped / undoped interface, and (II) creation of Ag^+ ions at the Ag / doped ChG interface were photogenerated holes, after the drift through doped layer react with neutral Ag atoms. In turn, Ag^+ ions after the drift towards the doped / undoped interface accept the unpaired electron from chalcogen dangling bond and a photodoped quaternary $Ag-As-S-Ge$ compound is created. Thus, the reaction limited stage of PD depends either on electronic (hole) photoconductivity of doped layer s_{ph} or on its ionic conductivity s_{Ag^+} . Effect of temperature on PD rate (here is not shown) indicates that the PD kinetics on the second step is a reaction limited process by photoconductivity s_{ph} , under condition that $s_{ph} \ll s_{Ag^+}$.

On the third step of PD kinetics the thickness of Ag film, being plotted versus square-root of exposure time shows linear dependences. The thickness change can be described by relation:

$$\Delta d_t = (2kt)^{\frac{1}{2}} \quad (2)$$

The values of parabolic constant k estimated from the slope of these curves are listed in Table 1. One can see that the values of k are in the range of $(0.33 - 3.5) \cdot 10^{-13} \text{ cm}^2 \text{ s}^{-1}$ reaching the maximal value for composition $(GeS_4)_{0,33}(AsS_3)_{0,67}$.

We assert that the maxima of both PD rate and of diffusion coefficient around composition $(GeS_4)_{0,33}(AsS_3)_{0,67}$ may be due to the change in the morphology of this glassy material i.e. its homogenization. A homogeneous backbone promotes the transport of both electrons and ions involved in photoreaction because of lack of phase boundaries and additional defects.

III. Conclusions

The PD kinetics profiles of Ag in glassy $(GeS_4)_x(AsS_3)_{1-x}$ films comprise two consecutive linear steps followed by a quasi-parabolic tail. The slope of the first step does not depend on composition. This step is ascribed to direct interaction of Ag with free sulfur of glassy material at the interface. The rate of PD on the second linear step, ascribed to photoconductivity limiting solid-state reaction, shows a maximum at $(GeS_4)_{0,33}(AsS_3)_{0,67}$. The diffusion coefficient, determined from the third, quasi-parabolic tail reaches its maximal value $\sim 3.5 \cdot 10^{-13} \text{ cm}^2/\text{s}$ by the same composition. It is assumed that this composition yield a homogeneous reaction product.

IV. References

1. A.V. Kolobov and S.R. Elliott, Photodoping of amorphous chalcogenides by metals, *Adv. Physics* 40 (1991) 625-684.
2. J. Ploccharski, J. Przulski and M. Teodorczyk, Ionic conductivity of Ag photodoped As_2S_3 glass, *J. Non-Cryst. Solids* 93 (1987) 303-310.
3. S.R. Elliott, A unified mechanism for metal photodissolution in amorphous chalcogenide materials, *J. Non-Cryst. Solids* 130 (1991) 85-97.
4. H.Jain, A Kovalskiy, A.Miller, An XPS study of the early stages of silver photodiffusion in Ag/a- As_2S_3 films *J. Non-Cryst. Solids* 352 (2006) 562-566.
5. D. Tsiulyanu and I. Stratan, On the photodissolution kinetics of silver in glassy As_2S_3 , *J. Non-Cryst. Solids* 356 (2010) 147-152.
6. I. An, H.Oh, Optical Properties of Silver Thin Films: Three-Parameter Spectroscopic Ellipsometry Studies, *Journ. Korean Phys. Society* 29 (1996) 370-376.
7. T. Kawaguchi, S. Maruno and S.R. Elliott, Optical, electrical and structural properties of amorphous Ag-Ge-S and Ag-Ge-Se films and comparison of photoinduced and thermally induced phenomena of both systems, *J. Appl. Phys.* 79 (1996) 9096-9104.
8. X. Sun, R. Hong, H. Hou, Z. Fan, J. Shao, Thickness dependence of structure and optical properties of silver films deposited by magnetron sputtering, *Thin Solid Films* 515 (2007) 6962-6966.
9. V. Balan, A. Piarristeguy, M. Ramonda, A. Pradel, M. Ribes, Phase separation and ionic conductivity: an electric force microscopy investigation of silver chalcogenide glasses, *J. Optoelectr. Adv. Matter.* 8 (2006) 2112-2116.

Acknowledgements

This work was supported by SCSTD of Academy of Sciences of Moldova, project 11.817.05.21A.